APPLICATION OF COMPUTATIONAL FLUID DYNAMICS FOR EVALUATION OF WIND POWER POTENTIAL IN SIMPLE TERRAIN

Tanit-Daniel Jodar Vecina
Department of Mechanical Eng., Faculty of Engineering, Universidade Federal do Rio Grande do Sul, Porto Alegre
jodar.vecina@ufrgs.br

José Leandro Rosales Luz
Department of Mechanical Eng., Faculty of Engineering, Universidade Federal do Rio Grande do Sul, Porto Alegre
jluz@mecanica.ufrgs.br

Gustavo Dias Fleck
Department of Mechanical Eng., Faculty of Engineering, Universidade Federal do Rio Grande do Sul, Porto Alegre
fleck@mecanica.ufrgs.br

Adriane Prisco Petry
Department of Mechanical Eng., Faculty of Engineering, Universidade Federal do Rio Grande do Sul, Porto Alegre
adrianep@mecanica.ufrgs.br

Abstract. *Computational 2D and 3D studies of the wind behavior flowing over hypothetical, symmetrical hills have been performed. The numerical simulations were performed using a commercial CFD code, which uses the Finite Volume Method to solve the conservation equations. The present work is divided in two cases: one two-dimensional, steady-state case in which the surface roughness is neglected, and one three-dimensional, in which subcases the use of surface roughness and the steady and transient regimes is alternated. The problem is solved with two different turbulence models, but only steady state is used. Also the surface roughness is considered in one of the cases. Throughout the study, both the k-ε e k-ω SST turbulence models were used. Results are presented so that comparisons between 2D and 3D simulations are favored. Those, in turn, are compared with experimental data provided by wind tunnel experiments.*

Keywords: *Atmospheric boundary layer; Wind Energy; Micrositing; Numerical Simulation; Computational Fluid Dynamics.*

1. INTRODUCTION

This paper presents a study on the use of Computational Fluid Dynamics (CFD) for the evaluation of wind energy potential on a simple terrain. In this case the flow is evaluated on two models of hypothetical symmetrical hills, a two-dimensional and three-dimensional with the same height and same dimensions, in order to compare the results between them focusing on determining the turbulence model that best suits the experimental study developed in the wind tunnel for (Mattuella, 2012).

The models are reduced to the same scale of the experiment in wind tunnel. SolidWorks was used to model the geometries computationally. The simulations are performed by employing two turbulence models and by varying the surface roughness values. The first case employed the k-ε turbulence model, widely used in specific wind simulation software (Fallo, 2007). Later simulations were performed using the SST k-ω turbulence model, also used to air flow studies over complex terrain (Wilcox, 1998) and (Silveira Neto, 2002).

Numerical simulations of the air flow over the terrain were performed using the ANSYS-Fluent 14.0 commercial code, which uses the finite volume method to solve the Reynolds-Averaged Navier-Stokes equations in steady state. Finally results are compared between the two dimensional and three dimensional models and different types of turbulence models and numerical schemes used. Results were compared with experimental data obtained in the wind tunnel for (Mattuella, 2012).

In one case the surface roughness is taken into account; the value used was the same as the one modeled at the experiments.

2. METHODOLOGY

This chapter presents the methodology used to perform the simulations. Initially is presented the issue to be reproduced numerically, followed by the description of the numerical methodology.

2.1 Definition of the problem

The problem to be assessed is the evaluation of the flow field over a scale model of a simple topological formation making use of the Computational Fluid Dynamics approach. The air flow will be characterized by the solution of the linearized Reynolds-Averaged Navier-Stokes (RANS) set of equations. The geometry consists of two symmetrical sinusoidal hypothetical models, a two-dimensional and three-dimensional, both with the same height and dimension. The models were analyzed individually and then their results were compared.

2.2 Models used

The numerical geometry reproduces the models used in the experiments. They are a 1:1000 scale representation of the hills and were tested at the Prof. Joaquim Blessmann Wind Tunnel (LAC, 2010). Figure 1 shows the two experimental models:

Figure 1. – Models used for the experimental tests conducted by Mattuella, 2012.

By the coordinates of the abovementioned hills, the computational geometric model was generated. This representation made in SolidWorks 2014 of scale models was performed in accordance with the wind tunnel measurements (LAC, 2010). Figure 2 represents the dimensions of the 2D hill.

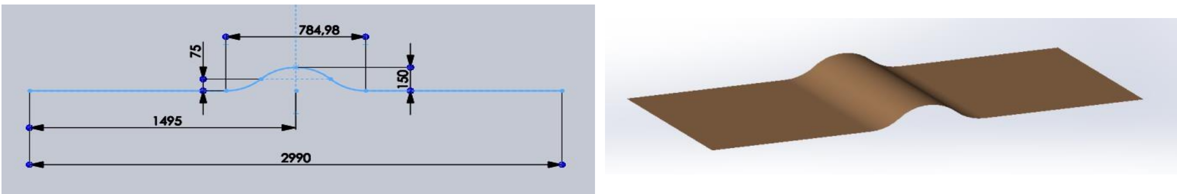

Figure 2 - Computational geometry of the 2D model.

Figure 3 representing the dimensions of the tridimensional hill:

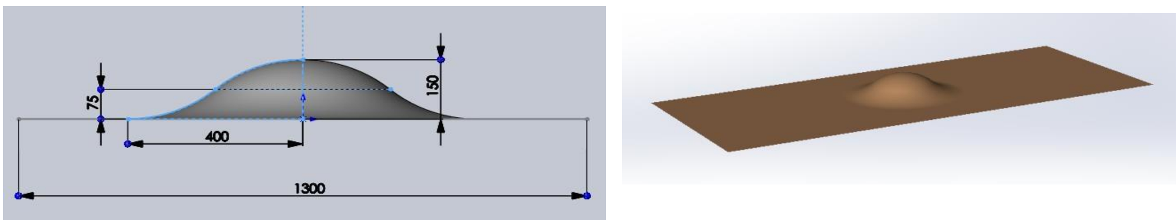

Figure 3 – Computational geometry of the 3D model.

2.3 Numerical Simulations

Two turbulence models are used, the k-ε, widely used in fluid dynamic studies and the k-ω SST, which has better performance in adverse pressure gradients (detachment of the CLA).

The simulations are performed in 3D through the ANSYS-Fluent 14.0 a RANS commercial code based on the Finite Volume Method (Maliska, 2004). The working fluid is air modeled as an incompressible ideal gas at 25°C. Heat transfer was not considered. The SIMPLE pressure-velocity coupling method was used, and the convergence criterion was set at $1x10^{-5}$.

2.4 Domain and discretizatio

The computational domain was discretized in small hexahedral volumes, in which the flow properties are evaluated at its centroids. The software used for the mesh generation was Ansys ICEM-14.0.

Refinement is heavier near the surface of the topology. For the two-dimensional hill, four meshes were created varying the number of cells, in order to evaluate the grid quality. Only one of them will be used for the final results. Details of the four meshes created for the domain are shown in Tab. 1:

Table 1 – Volume count for the meshes contemplating the two-dimensional hill.

	ELEMENTS X	***ELEMENTS Y***	***ELEMENTS Z***	***Nº VOLUMES***
CASE 1	100	25	25	59.212
CASE 2	250	60	60	804.375
CASE 3	300	75	75	1.665.000
CASE 4	320	90	90	2.200.000

The volumes in the X direction (from the inlet towards the outlet were divided into three zones: the foremost zone, containing the inlet of the velocity profile) and the last zone, containing the outlet, have the same number of volumes and equal spacing in relation to the center region. The mesh in this center region has a superior refinement, due to being the zone of greater interest towards the results. Uniform volume density was set in the Y (height) and Z (width) directions. Figure 4 shows one of the meshes, in which the domain divisions can be identified.

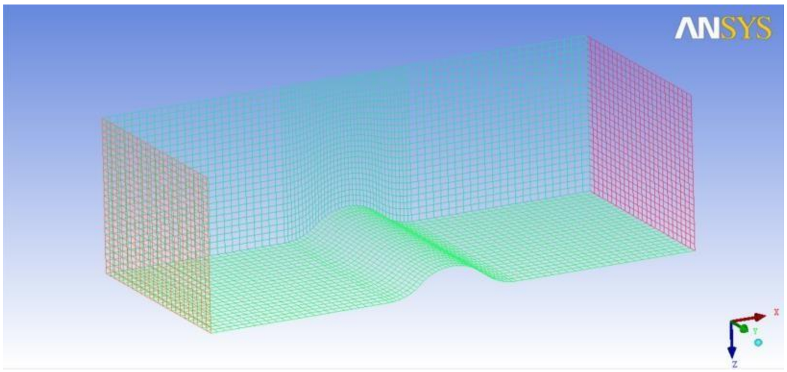

Figure 4 – View of one of the discretization meshes. Note the domain subdivisions.

For the discretization of the three-dimensional hill, four meshes were created using the same methodology as for the two-dimensional case. Thus, the domain was discretized as shown in Tab. 2:

Table 2 – Volume count for the meshes contemplating the three-dimensional hill.

	ELEMENTS X	***ELEMENTS Y***	***ELEMENTS Z***	***Nº VOLUMES***
CASE 1	100	30	30	150.000
CASE 2	150	50	50	375.000
CASE 3	250	75	75	1.406.250
CASE 4	275	85	85	1.986.875

The meshes for this case were created in a similar fashion as for the two-dimensional hill. They have the same number of elements in the directions Y and Z. Element distribution in the X and Y axes is uniform, but the grids have a higher refinement close to the surface of the hill, thus showing an uneven distribution. This distribution follows an exponential law. The grid generated and a heavier volume density near the hill surface can be seen in Fig. 5

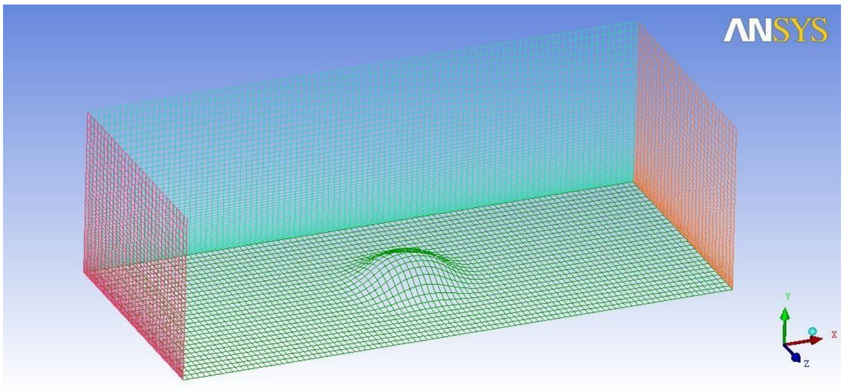

Figure 5 - View of one of the discretization meshes. Note the heavier refinement close to the base of the domain.

2.5 Boundary conditions

A velocity profile with the same characteristics as the one used at the experiments was used in the simulations, focusing on reproducing the experimental tests as accurately as possible. According to data provided by LAC, 2010, the bottom of the tunnel elements have a roughness such that the power law is expressed with p = 0.23. The upper part elements have no roughness, so that a value of p = 0.11 for the velocity profile is used in this region. The equations that represent this modeling are shown as follows:

$$\frac{U}{U_{(0.8)}} = 1 - \left| \left(\frac{z-0.8}{0,8} \right)^{0.23} \right| \qquad 0 < z < 0.8 \qquad (1)$$

$$\frac{U}{U_{(0.8)}} = 1 - \left| \left(\frac{z-0.8}{0.8} \right)^{0.11} \right| \qquad 0.8 \leq z < 0.9 \qquad (2)$$

U is the free stream velocity and $U_{(0.8)}$ is the velocity at a reference height (in this case 0.8 m). The inlet boundary condition was modeled as a velocity profile by the abovementioned equations and was applied into ANSYS Fluent by means of the User-Defined Function (UDF) option. This function allows the user to implement any profile, since the function is written in C language. The mathematical modeling described by Eqs. (1) and (2) represents the X-component of the inlet velocity. Y and Z components were set up at the value of zero.

The output boundary condition is prescribed atmospheric pressure over the whole outlet surface. This option is used when the flow pressure and velocity fields at the outlet are unknown.

No-slip condition was prescribed to all walls of the domain, including the sidewalls and the upper part. The tunnel walls are made of wood, so the prescribed roughness set for wood is 0.0009 meters.

The tunnel ground was modeled as no-slip wall as well, but special attention must be given to the region of the topologies. The presence or absence of roughness over the hills depends on the case simulated.

3. RESULTS

Firstly, the evaluation of the mesh quality was carried out. This is probably one of the most important parts of this work. The reliability of the results depends directly on this factor. The study is divided into two cases:

The first case focuses on the model containing the two-dimensional hill, also called "2D", which is used for two types of simulation: the first where the surface roughness is neglected and where the k-ε turbulence model is used in steady state; the second resolution uses the SST k-ω turbulence model in steady state.

The second case focuses on the three-dimensional hill model or "3D". This case is divided into three types of resolution. In the first and second cases the roughness is neglected, but in the third case it is considered as a surface roughness equivalent to that used for the experimental assessment. In the first simulation, the k-ε turbulence model was used in steady state. In the second simulation the model used was the SST k-ω and it is the same as above, it is solved in steady state. In the latter one, the roughness resolution is taken into account, and the problem is solved using the SST k- ω model. The solution is obtained in steady state.

Table 3 presents all the cases assessed in the following chapters of the present work.

Table 3 – Description of the cases assessed in the present study.

Case		Regime	Turbulence model
I	2D	*Steady*	*k-ε*
II			SST *k-ω*
III	3D	*Steady*	*k-ε*
IV			SST *k-ω*
V			SST *k-ω* w/ roughness

3.1 Grid quality evaluation

The grid quality study was performed through the observation of the Wind velocity right over the considered topology, where na incremente in the flow speed can be detected. The study takes into account the number of volumes of each mesh. Simulations were performed with the 2D and 3D grid cases, all of them with the *k-ε* turbulence model in steady state.

Table 4 – Grid independence results for the 2D hill model.

	N° NODES	VELOC. [M/S]	VAR. (%)
GRID 1	59.212	10,9623	-
GRID 2	804.375	10,9220	0,3676
GRID 3	1.665.000	10,9121	0,0906
GRID 4	2.200.000	10,9086	0,0320

Results show that there is little velocity variation at the point considered; the difference is under 1% for all cases. Nevertheless, grid 3, which has about 1.5 million volumes, was chosen to be used on further simulations. This is due to the fact that grid 3 presents the best balance between computational time and precision of the results. Grid 4 was discarded due to the lack of significant precision on its results that justify its higher computational time.

Table 4 shows the velocity results at the point X,Y,Z = (0, 0, 180 mm) and its variation as a function of the number of volumes of the mesh for the 3D case.

Table 5 – Grid independence results for the 3D hill model.

	N° NODES	VELOC. [M/S]	VAR. (%)
GRID 1	150.000	9,41051	-
GRID 2	375.000	9,48421	0,7639
GRID 3	1.406.250	9,52127	0,3907
GRID 4	1.986.875	9,53152	0,1076

From the analysis of the numbers from Tab. 5 it is possible to assert that the wind velocity at the considered location also presents small variation. Thus, the results delivered by any of the four grids can be stated as correct for this study. Similarly to the previous case, and for the same reason, mesh 3 was again selected to be used on further simulations for the 3D hill case.

3.2 Flow over the 2D hill surface

Results obtained in the cases I and II (according to Tab. 3), the airflow on the two-dimensional model, are presented below. The roughness is neglected for all cases of the 2D hill.

Figure 6 shows the contours of the velocity field in the longitudinal plane of the domain. The air flow, represented by a prescribed velocity profile, enters at the left side of the pictures. The velocity field remains constant at the first stretch of the domains. At the top of the hill there is a region with a substantial increase in speed, this acceleration occurs due to reduction of the air passage area, so that there is compensation speed thereof, i.e., the ridge acts as a concentrator of air streamlines, accelerating the wind [Luz, 2009].

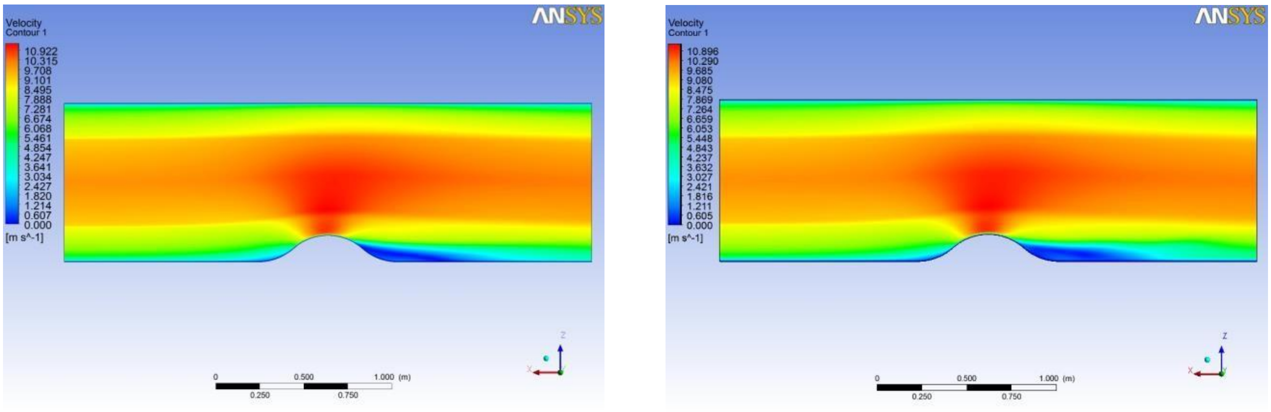

Figure 6 – Air flow over the two-dimensional hill. (a) Turbulence model *k-ε and (b)* Turbulence model SST *k-ω*.

Figure 7(a) shows the velocity variation as a function of the longitudinal distance X to a fixed heigth Z = 250 mm. the velocity at the domain entry is 9,4 m/s due to the prescribed profile, and it grows exponentially along the flow direction up to reaching the maximum speed. This speed is approximately 10,8 m/s and is located at 1500 mm from the inlet.From this point on, speed starts to decrease, also exponentially, up to reaching 9,6 m/s. it is worth noting that the velocity difference between the results of both models is very small regarding to the inlet, outlet and maximum speeds. As can be seen in the graph, velocity results from the SST *k-ω* model are slightly lower than those produced by the *k-ε* model.

Figure 7(b) shows how the velocities vary depending on the vertical Z distance at the center of the domain, X, Y = (0,0). It is possible to see that at Z = 150 mm (corresponding to the top of the hill) the flow velocity is zero, and it grows to its maximum value of 11,25 m/s along the vertical line at Z = 310 mm, or 160 mm above the top of the hill. From this point on, the velocity starts to decrease up to reaching 0 m/s. This is due to the fact that at the last 100 mm of the domain height the velocity profile is represented by the Equation (2), having an exponent smaller than that used in Eq. (1), which represents the initial 800 mm. Besides that, the hill does not influence the flow significantly at the very top of the domain, and the domain ceiling has the no-slip condition, which forces the flow to come to a stop there.

Analysis shows no significant differences between the results of both turbulence models.

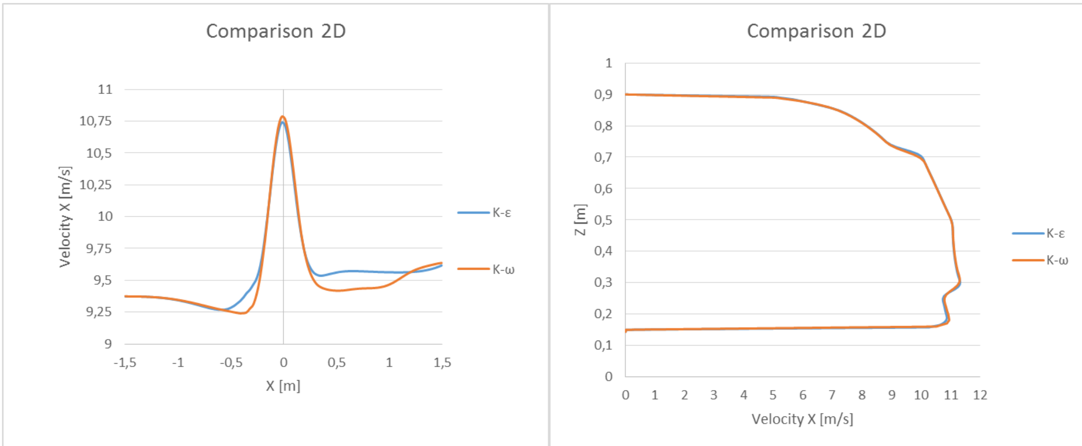

Figure 7 (a) 7 (b) – Comparison of turbulence models.

3.3 Flow over the 3D hill surface

Below are presented the results of the cases III to V (according to Tab. 3), of the airflow on the three-dimensional model. In the following cases the velocity profile enters at the left side of the images. On the home stretch the velocity field remains constant up to focus on the hill, where it starts to increase the value of the velocity field. The top of the hill has a region with a considerable increase in speed due to wind collision. The above explanation is valid for all following cases regardless of the turbulence model or system. On the back of the hill there is a reduction in speed, this is caused by an adverse pressure gradient that causes the detachment of the boundary layer, this phenomenon is also called recirculation. This region after the hill is where changes happen; it depends on the turbulence model used.

Figure 8 shows the velocity field in the longitudinal plane of the domain for the cases III and IV.

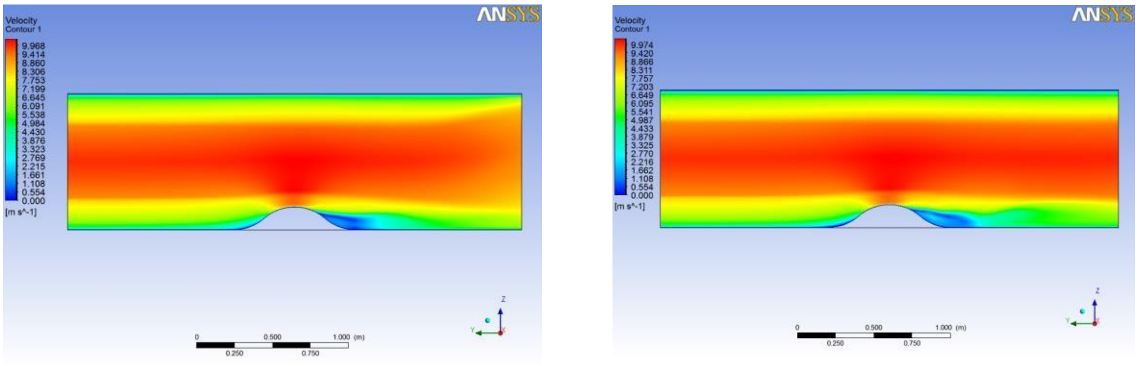

Figure 8 – Velocity contour (a) (a) Turbulence model *k-ε and (b)* Turbulence model SST *k-ω.*

Finally, case V is shown in Fig. 9. It is the only case where the roughness is considered and the value of roughness is the same as the wind tunnel case in order to then make a comparison of the results with the experimental data.

In the first stretch the velocity field remains constant up the hill from the start, even if in the previous cases, where it starts to increase the value of the velocity field. At the top of the hill has the maximum field speed, the explanation is the same as in the section 3.2. On the backside of the hill a reduction on the speed is observed, which is caused by the effect of recirculation, it can be seen how the model with roughness shows a more pronounced flow disturbance at the back of the hill.

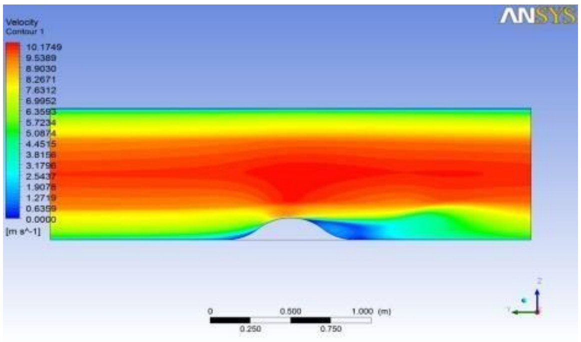

Figure 9 – Velocity contour Turbulence model SST *k-ω with roughness.*

Figure 10 (a) shows how the wind speed varies depending on the longitudinal distance X of the domain to a fixed height of Z = 250 mm. the velocity at the entry of the domain is about 9.4 m/s for all the cases due to the inlet velocity profile. Regarding to the turbulence models, differences between both of them occur due to the presence of the topology. SST *k-ω* produces a top speed of 10.2 m/s. *k-ε* gives a top speed of 10.15 m/s. Also, it is given speed downstream is smaller than that from the SST model. This is due to the SST model capabilities of calculating more precisely the velocities near the surfaces. Regarding to the simulations performed with the presence of roughness, a stronger recirculation is noticed downstream from the hill.

Figure 10 (b) shows the behavior of the velocity as a function of the vertical Z distance from the hill at the midpoint X,Y = (0,0). Analysis of the figure shows that the flow speed varies from zero at the top of the hill to a maximum value of 10.3 m/s at Z = 260 mm, then it decreases and grows again to the maximum value abovementioned at Z = 400 mm. The speed then decreases again up to the value of zero at the very top of the domain, due to the presence of the no-slip wall.

The only significant difference among the simulations is that the SST *k-ω* with roughness shows a value for the wind speed lower than the other cases between Z = 150 mm and 210 mm. The difference is around 0.5 m/s.

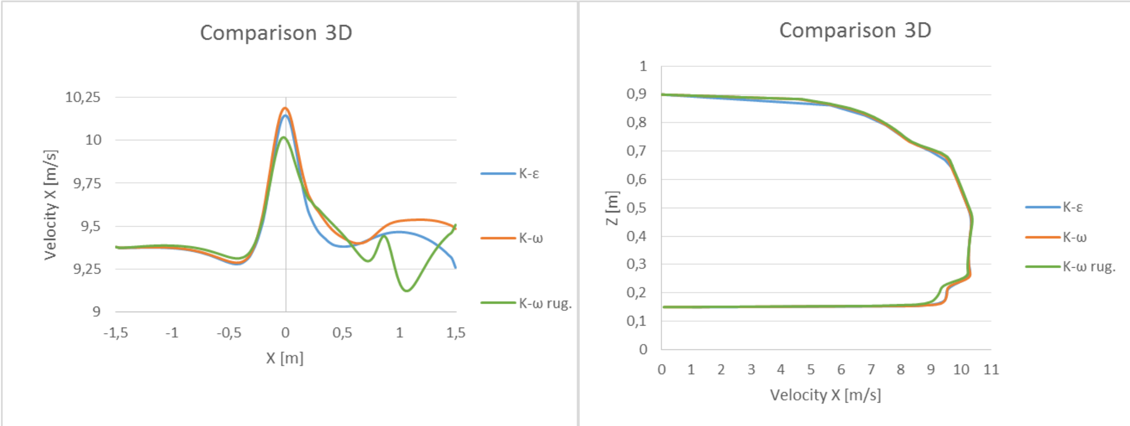

Figure 10 - Comparision of turbulence models.

3.4 CFD Vs. Experimental

This comparison is performed through the analysis of Fig. 11, which shows the comparison, among the 3D models, of the normalized velocities at Z = 250 mm from the top of the hill.

Once visualized the above graph it is clear that there is no difference between the two turbulence models, where if you only choose the k-ω SST to put the roughness.

While turbulence models K ω-SST with no roughness and surface roughness shows a difference in the first 100 mm, the specimen is neglected roughness shows a higher speed on this stretch values. This is because the roughness decreases the wind velocity near the surface. In relation to the experimental model, the model results with these first beat roughness 100 mm in leg 100 to 200 mm, the experimental model presents a lower speed than in the simulated model. After the 200 mm to 350 mm speeds become identical again. Finally in the last 100 mm experimental study speed becomes greater than the sham. This may be because in the case simulated the velocity profile presents a different exponent in the last 100 mm of the domain and also has the wall condition in the higher plane of said domain.

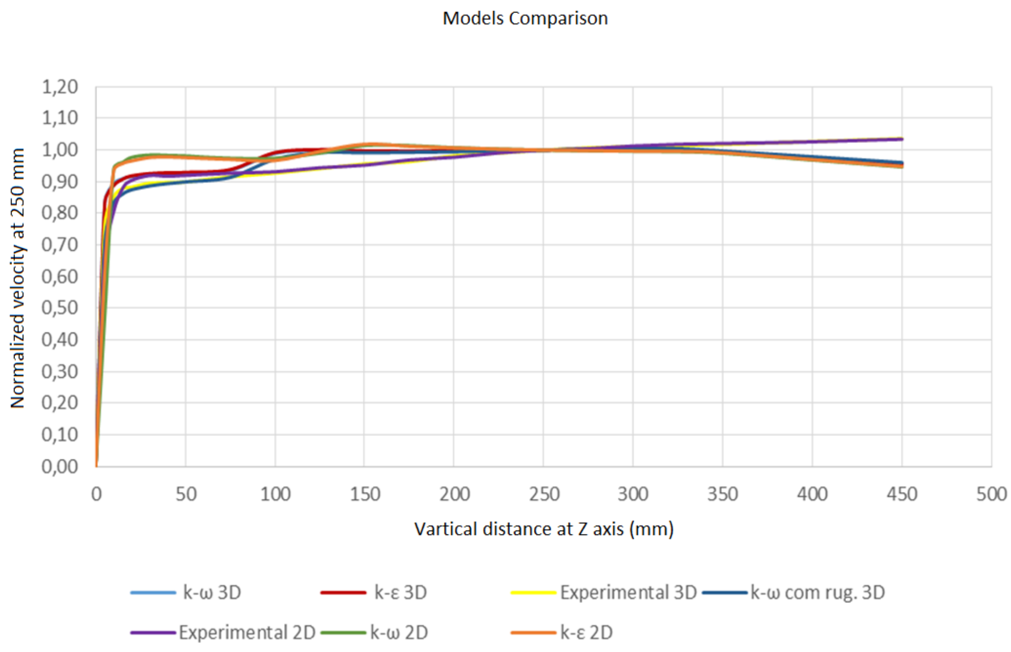

Figure 11 – Comparison of Turbulence models and experimental results.

4. CONCLUSIONS

In the 2D model, there is a strong similarity between the numerical results obtained by both turbulence models. In relation to the experimental data, the average difference in a place considered as no more than 6%. Regarding the 3D model, the analysis of the numerical simulations velocity fields allows to note differences in flow behavior, especially downstream of the obstacle.

Comparing the numerical results, it is noted that the k- ω SST model results show a better agreement with the experimental roughness geometry was used exclusively with the first model. Despite the good agreement was found that numerical velocity even between 350 and 450 mm the opposite occurs, and the calculated speed data is smaller than experimental. This may reflect the entry into force of the exponent p=0.11 in the last 100 meters of the field in the simulations, while in the experimental case this exponent remains fixed at 0.23 for any distance.

5. REFERENCES

Fallo, D. Wind Energy Resource Evaluation in Site of Central Italy by CFD Simulations. UNIVERSITÀ DEGLI STUDI DI CAGLIARI. Cagliari, Italia 2007.

Wilcox, D.C. Turbulence Modeling for CFD. DCW Industries, Anaheim, CA – USA, 1998.

Silveira Neto, A. D. Fundamentos da Turbulência em Fluidos. In Freire, A. P. S.; Menut, P. P. M.; Su,J.

Turbulência. Rio de Janeiro: ABCM, 2002.

LAC, LABORATÓRIO DE AERODINÂMICA DAS CONSTRUÇÕES. Relatório Interno de Medições morro

Jaburu em Vitória- ES. UFRGS, Porto Alegre, 2010.

Maliska, C.R. Transferência de calor e mecânica dos fluidos computacional. LTC 2004

Luz, J. L. R., Análise da influência de uma turbina eólica instalada em um morro no escoamento dos ventos utilizando dinâmica dos fluidos computacional. UFRGS, Porto Alegre, 2009.

6. RESPONSIBILITY NOTICE

The authors are the only responsible for the printed material included in this paper.